Molecular Pharmacology Fast Forward. Published on January 31, 2023 as DOI: 10.1124/molpharm.122.000589
This article has not been copyedited and formatted. The final version may differ from this version.

The Small Molecule Antagonist KCI807 Disrupts Association of the Amino-terminal Domain of the Androgen Receptor with ELK1 by Modulating the Adjacent DNA Binding Domain

Claire Soave, Charles Ducker, Naeyma Islam, Seongho Kim, Sally Yurgelevic, Nathan I. Nicely, Luke Pardy, Yanfang Huang, Peter E. Shaw, Gregory Auner, Alex Dickson and Manohar Ratnam

Department of Oncology, Wayne State University School of Medicine and Barbara Ann Karmanos Cancer Institute, Detroit, Michigan (C.S., S.K., Y.H., L.P. and M.R.)

Department of Biochemistry and Molecular Biology, College of Natural Science, Michigan State University, East Lansing, Michigan (N.I. and A.D.)

Smart Sensors and Integrated Microsystems (SSIM) Program, Wayne State University School of Medicine and Barbara Ann Karmanos Cancer Institute, Detroit, Michigan (S.Y. and G.A.)

School of Life Sciences, University of Nottingham, Queens Medical Centre, Nottingham, United Kingdom (C.D. and P.E.S.)

Department of Pharmacology, UNC-Chapel Hill School of Medicine, Chapel Hill, North Carolina (N.N.)

Downloaded from molpharm.aspetjournals.org at ASPET Journals on July 7, 2023

Molecular Pharmacology Fast Forward. Published on January 31, 2023 as DOI: 10.1124/molpharm.122.000589
This article has not been copyedited and formatted. The final version may differ from this version.

Running title: The binding site for KCI807 in the androgen receptor

Corresponding author: Manohar Ratnam

Address: 4100 John R Street, HWCRC Rm. 840.1, Detroit, MI 48201

Telephone: (313) 576-8612

Fax: (313) 576-8299

E-mail: ratnamm@karmanos.org

Number of text pages: 38

Number of tables: 0

Number of figures: 7

Number of references: 41

Number of words in Abstract: 250

Number of words in Introduction: 749

Number of words in Discussion: 1334

Abbreviations:

AR: Androgen receptor

AR-V7: Androgen receptor splice variant 7

KCI807: 5-hydroxy-2-(3-hydroxyphenyl)chromen-4-one

PCa: Prostate cancer

NTD: Amino-terminal domain

DBD: DNA binding domain

Downloaded from molpharm.aspetjournals.org at ASPET Journals on July 7, 2023

Molecular Pharmacology Fast Forward. Published on January 31, 2023 as DOI: 10.1124/molpharm.122.000589
This article has not been copyedited and formatted. The final version may differ from this version.

LBD: Ligand binding domain

ETS: Erythroblast transformation specific

ERK: Extracellular signal-regulated kinase

MEK: Mitogen activated protein kinase kinase

GST: Glutathione S-transferase

Downloaded from molpharm.aspetjournals.org at ASPET Journals on July 7, 2023

Molecular Pharmacology Fast Forward. Published on January 31, 2023 as DOI: 10.1124/molpharm.122.000589
This article has not been copyedited and formatted. The final version may differ from this version.

Abstract

The androgen receptor (AR) is a crucial coactivator of ELK1 for prostate cancer (PCa) growth, associating with ELK1 through two peptide segments (358-457 and 514-557) within the amino-terminal domain (NTD) of AR. The small-molecule antagonist KCI807 binds to AR, blocking ELK1 binding and inhibiting PCa growth. We investigated the mode of interaction of KCI807 with AR using systematic mutagenesis, coupled with ELK1 coactivation assays, testing polypeptide binding and Raman spectroscopy. In full-length AR, deletion of neither ELK1 binding segment affected sensitivity of residual ELK1 coactivation to KCI807. Although the NTD is sufficient for association of AR with ELK1, interaction of the isolated NTD with ELK1 was insensitive to KCI807. In contrast, coactivation of ELK1 by the AR-V7 splice variant, comprising the NTD and the DNA binding domain (DBD), was sensitive to KCI807. Deletions and point mutations within DBD segment 558-595, adjacent to the NTD, interfered with coactivation of ELK1, and residual ELK1 coactivation by the mutants was insensitive to KCI807. In a GST pull-down assay, KCI807 inhibited ELK1 binding to an AR polypeptide that included the two ELK1 binding segments and the DBD but did not affect ELK1 binding to a similar AR segment that lacked the sequence downstream of residue 566. Raman spectroscopy detected KCI807-induced conformational change in the DBD. The data point to a putative KCI807 binding pocket within the crystal structure of the DBD and indicate that either mutations or binding of KCI807 at this site will induce conformational changes that disrupt ELK1 binding to the NTD.

Downloaded from molpharm.aspetjournals.org at ASPET Journals on July 7, 2023

Molecular Pharmacology Fast Forward. Published on January 31, 2023 as DOI: 10.1124/molpharm.122.000589
This article has not been copyedited and formatted. The final version may differ from this version.

Significance statement: The small-molecule antagonist KCI807 disrupts association of the androgen receptor (AR) with ELK1, serving as a prototype for the development of small molecules for a novel type of therapeutic intervention in drug-resistant prostate cancer. This study provides basic information needed for rational KCI807-based drug design by identifying a putative binding pocket in the DNA binding domain of AR through which KCI807 modulates the amino-terminal domain to inhibit ELK1 binding.

Downloaded from molpharm.aspetjournals.org at ASPET Journals on July 7, 2023

Molecular Pharmacology Fast Forward. Published on January 31, 2023 as DOI: 10.1124/molpharm.122.000589
This article has not been copyedited and formatted. The final version may differ from this version.

Introduction

The mainstay treatment for management of advanced PCa is testosterone suppression, achieved by a combination of chemical castration, inhibition of residual testosterone synthesis, and androgen antagonists (Dunn and Kazer, 2011; Loblaw et al., 2007; Teo et al., 2019). Resistance to testosterone suppression is commonly due to restoration of androgen receptor (AR) function by overexpression of AR, expression of AR splice variants that do not bind hormone, AR mutations, activation of AR by hormone-independent phosphorylation, and alterations in AR co-regulators (Henzler et al., 2016; Hu et al., 2012; Koryakina et al., 2014; Li et al., 2013; Nyquist et al., 2013; Sun et al., 2010; Visakorpi et al., 1995). There is thus a need to develop drug molecules that will disrupt hormone-independent aspects of AR function (Li et al., 2014; Monaghan and McEwan, 2016; Monaghan et al., 2022; Radaeva et al., 2021).

AR is a ~920 amino acid polypeptide containing an amino-terminal A/B domain (NTD) followed in sequence by a DNA binding domain (DBD), a hinge region, and a ligand (hormone) binding domain (LBD) (MacLean et al., 1997). The NTD includes a ligand-independent transcriptional activation function (AF1), comprising two units, TAU1 and TAU5 (Christiaens et al., 2002). The LBD contains a ligand-dependent transcriptional activation function, AF2 (Bevan et al., 1999). Androgen binding to the LBD enables AR to translocate to the nucleus; however, splice variants lacking this domain do induce androgen response genes and support growth in a hormone-independent manner (Henzler et al., 2016; Hu et al., 2012; Kounatidou et al., 2019; Li et al., 2013; Nyquist et al., 2013; Sun et al., 2010).

We have shown that the ETS family transcription factor ELK1 is essential for growth and tumorigenicity, selectively in AR-dependent PCa cells, including those resistant to currently used

Downloaded from molpharm.aspetjournals.org at ASPET Journals on July 7, 2023

Molecular Pharmacology Fast Forward. Published on January 31, 2023 as DOI: 10.1124/molpharm.122.000589
This article has not been copyedited and formatted. The final version may differ from this version.

AR antagonists (Patki et al., 2013). AR is a transcriptional coactivator of ELK1 (Patki et al., 2013). ELK1 binds to purine-rich GGA core sequences in the DNA and is classically transiently activated upon phosphorylation by ERK (Extracellular signal-regulated kinase) at multiple carboxy-terminal sites (Gille et al., 1992; Shaw and Saxton, 2003; Zhang et al., 2008). In its basal state, ELK1 either represses or is passively associated with its target genes, which support cell cycle progression and mitosis (Gille et al., 1992; Shaw and Saxton, 2003; Zhang et al., 2008). AR binding sites in the chromatin are highly enriched for ELK1 binding (Yu et al., 2010). ELK1 is at least partially required for constitutive activation by AR of about a third of AR target genes, primarily those required for cell proliferation (Patki et al., 2013; Rosati et al., 2016). Activation of ELK1 target genes by AR as a coactivator of ELK1 does not require phosphorylation of ELK1, or even the transactivation domain of ELK1 (Patki et al., 2013; Rosati et al., 2016). AR binds to ELK1 (Kd = 1.9 x 10^{-8} M) through AR's NTD, by co-opting the two ERK docking sites in ELK1 (Rosati et al., 2016). Direct binding of AR to ELK1 is necessary for PCa cell growth; a docking site mutant of ELK1 has a dominant-negative effect on growth in PCa cells that are insensitive to inhibition of MEK (Rosati et al., 2016). We have recently mapped the ELK1 recognition sites in AR to two peptide segments within the NTD, spanning amino acids 358-457 and 514-557 (Soave et al., 2022). ELK1 is an independent prognosticator of PCa recurrence (Pardy et al., 2020) and the AR-ELK1 axis is a validated target for the development of novel therapeutics to treat advanced prostate cancer resistant to hormone-based therapies (Rosati et al., 2018).

KCI807 is a small molecule inhibitor of the AR-ELK1 interaction and a novel AR antagonist, based on its target selectivity, binding affinity, biological selectivity and efficacy (Rosati et al., 2018). KCI807 bound to AR (Kd = 7 x 10^{-8} M) and blocked the association of

Downloaded from molpharm.aspetjournals.org at ASPET Journals on July 7, 2023

Molecular Pharmacology Fast Forward. Published on January 31, 2023 as DOI: 10.1124/molpharm.122.000589
This article has not been copyedited and formatted. The final version may differ from this version.

ELK1 (Rosati et al., 2018). KCI807 selectively prevented recruitment of AR to chromatin sites by ELK1 but did not interfere with the binding of AR to canonical androgen response elements (AREs) (Rosati et al., 2018). The KCI807 target genes virtually exclusively comprised genes that were synergistically activated by ELK1 and AR (Rosati et al., 2018). KCI807 selectively inhibited growth of AR-dependent PCa cells, including enzalutamide-resistant cells, and suppressed *in vivo* growth of enzalutamide-resistant PCa tumor xenografts including patient-derived tumors (Rosati et al., 2018).

Here we use KCI807 as the prototype antagonist of the association of AR with ELK1 to identify its binding site within AR and to understand the mechanism by which it disrupts the ELK1-AR complex.

Downloaded from molpharm.aspetjournals.org at ASPET Journals on July 7, 2023

Molecular Pharmacology Fast Forward. Published on January 31, 2023 as DOI: 10.1124/molpharm.122.000589
This article has not been copyedited and formatted. The final version may differ from this version.

Materials and Methods

Cell Lines and Reagents

HeLa-HLR cells were kindly provided by Dr. Johann Hofmann (Innsbruck Medical University). These recombinant HeLa cells harbor a TATA box-dependent basal promoter with upstream Gal4 elements and a luciferase reporter (*GAL4-TATA-LUC*). HeLa-HLR cells also constitutively express the Gal4-ELK1 fusion protein, in which the ETS DNA binding domain of ELK1 is replaced by the Gal4 DNA binding domain. HeLa-HLR cells were grown in DMEM supplemented with 10% FBS and 100 units/mL penicillin, 100 µg/mL streptomycin, 2 mM L-glutamine mixture (Invitrogen). In addition, the culture media for HeLa-HLR cells included the antibiotics, hygromycin (100 µg/mL) (10687010, Invitrogen) (to select for Gal4-ELK1) and geneticin (100 or 400 µg/mL) (10131027, Invitrogen) (to select for *GAL4-TATA-LUC)*. Rabbit monoclonal antibody to AR (ab133273, RRID: AB_11156085) (1:500 dilution) was bought from Abcam. Antibody to GAPDH (sc-47724, RRID: AB_627678) (1:3000 dilution) was bought from Santa Cruz Biotechnology. Lipofectamine-2000 (11668027) was bought from Invitrogen. KCI807 (5,3'-dihydroxyflavone or 5-hydroxy-2-(3-hydroxyphenyl)chromen-4-one) was ordered from Indofine. All cultured cells were of early passage that tested free of mycoplasma contamination.

Purified Proteins

Human ELK1-His was recombinantly expressed from baculovirus-infected Sf9 cells and purified by nickel affinity chromatography, eluted with 200mM imidazole (in 50mM Na_2HPO_4/NaH_2PO_4

Downloaded from molpharm.aspetjournals.org at ASPET Journals on July 7, 2023

Molecular Pharmacology Fast Forward. Published on January 31, 2023 as DOI: 10.1124/molpharm.122.000589
This article has not been copyedited and formatted. The final version may differ from this version.

pH 7.0) and dialyzed against 20 mM HEPES-NaOH (pH 7.9), 10% glycerol, 20 mM KCl, 2 mM $MgCl_2$, 0.2 mM EDTA, 0.5 mM benzamidine and 0.5 mM DTT. GST-tagged human AR334-566 and AR328-631 were expressed from Rosetta(DE3) *E. coli* cells and purified by glutathione-sepharose affinity chromatography, eluted with 10 mM reduced glutathione and dialyzed against HBS-N (10 mM HEPES-NaOH pH 7.4, 150 mM NaCl) supplemented with 0.2 mM EDTA and 1mM DTT. The rat AR polypeptide 491-679, which contains within it a sequence identical to that of the human AR DNA binding domain (DBD) (amino acids 558-624 in human AR, corresponding to amino acids 540-606 in rat AR) and some flanking sequences extending into the upstream NTD and downstream hinge region that are entirely non-homologous to human AR, was purchased from Abbexa.

Plasmids.

The pSG5-VP16-AR(A/B) plasmid, which expresses the hybrid polypeptide of VP16 and the NTD of AR, was previously constructed in our laboratory. The expression plasmid for AR (pSG5-hAR) was a kind donation from Lirim Shemshedini (University of Toledo, Toledo, OH). The pLVX-AR-V7 plasmid and pLVX control plasmid were kind gifts received from Dr. Yan Dong, Tulane University (New Orleans, LA). For protein expression, pGEX4T1-AR334-566 was obtained from Addgene (104198) and pGEX4T1-AR328-631 was constructed for this study, while pFastbac1-ELK1-His was constructed previously.

Generation of Mutant AR Constructs

To generate expression plasmids for mutant AR constructs, we used either the QuikChange II-XL Site-Directed Mutagenesis kit (200522) from Agilent or the Q5 Site-Directed Mutagenesis

Downloaded from molpharm.aspetjournals.org at ASPET Journals on July 7, 2023

Molecular Pharmacology Fast Forward. Published on January 31, 2023 as DOI: 10.1124/molpharm.122.000589
This article has not been copyedited and formatted. The final version may differ from this version.

kit (E0554S) from New England Biolabs and followed the manufacturer's instructions. The pSG5-hAR expression plasmid was used as the PCR template for all constructs except in the generation of the double deletion construct in which residues 358-459 and 514-557 were deleted; in this case, the template used was the AR construct containing the single deletion of residues 358-459. The primer sequences for all mutagenesis constructs are provided in the Supplement (Supp. Table 1).

Transfections and Reporter Luciferase Assays

Twenty-four hours prior to transfection, HeLa-HLR cells were plated at 100,000 cells/well in a 24-well plate in phenol red-free DMEM supplemented with 10% FBS and 2 mM L-glutamine. The cells were transfected using Lipofectamine-2000 (1:5 DNA:Lipofectamine-2000 ratio). After 48 hours, the cells were lysed with either Luciferase Assay Lysis Buffer 5X (E291A) or Cell Culture Lysis Buffer 5X (E1531) from Promega, following the manufacturer's protocol. The substrate for firefly luciferase provided in the Luciferase Assay System (E1501, Promega) was used to measure luciferase activity, using the LB 960 Centro XS^3 microplate luminometer (Berthold). IC_{50} values for inhibition of promoter activity by KCI807 were calculated using GraphPad Prism 5 software.

Western Blot Analysis

The samples for western blot were prepared by lysing cells using radioimmune precipitation assay buffer (150 mM NaCl, 1% Nonidet P-40, 0.5% sodium deoxycholate, 0.1% SDS, 50 mM Tris-HCl pH 8.0) which contained a protease inhibitor mixture and EDTA (78410, Thermo Fisher Scientific), and incubating on ice for 1 hour. Protein concentration was measured using

Downloaded from molpharm.aspetjournals.org at ASPET Journals on July 7, 2023

Molecular Pharmacology Fast Forward. Published on January 31, 2023 as DOI: 10.1124/molpharm.122.000589
This article has not been copyedited and formatted. The final version may differ from this version.

the Bradford assay (500006, Bio-Rad). The lysed samples were heated for 5 min at 95°C. Proteins (2-5 µg) in the samples were separated by electrophoresis on 8% SDS-polyacrylamide gels and electrophoretically transferred to PVDF membranes (IPVH00010, Millipore). The blots were probed with primary antibody and secondary horseradish peroxidase-conjugated antibody. Proteins were visualized using the WesternBright ECL Spray (K-12049-D50, Advansta) and a ChemiDoc Touch Imaging System (Bio-Rad).

GST Pulldown Assay

Pre-blocked (0.1% BSA) glutathione sepharose beads in HBS-N (supplemented with 0.1% Triton X-100) were incubated with 1.5µg GST/GST AR334-566/GST AR328-631 and 1µM KCI807 or vehicle (DMSO) for 1 hour at room temperature. ELK1-His was added (1µg) and beads were incubated for a further hour at room temperature, before being washed with HBS-N three times and resuspended in SDS loading buffer for western blot analysis.

Raman Spectroscopy

The samples were prepared in phosphate buffered saline. The AR DBD polypeptide used was a commercially available rat AR polypeptide which comprises a DBD sequence that is identical to the human AR DBD and flanking short non-homologous peptide sequences. The samples contained individually or in combination, AR DBD polypeptide (2 µM), KCI807 (2 µM) and the vehicle for KCI807 (DMSO at a final concentration of 0.02 percent). When protein and KCI807 or vehicle were combined, the sample was incubated for at least 3 minutes for the binding to be complete, based on previously published data on the rate of binding of the compound to AR (Rosati et al., 2018). For data acquisition, a 100 µL drop of each sample was placed on a

Downloaded from molpharm.aspetjournals.org at ASPET Journals on July 7, 2023

Molecular Pharmacology Fast Forward. Published on January 31, 2023 as DOI: 10.1124/molpharm.122.000589
This article has not been copyedited and formatted. The final version may differ from this version.

polished stainless steel slide. Using a Leica 63x dipping objective, spectra were acquired using a Renishaw inVia Raman Microscope equipped with a 514 nm laser, 1800 l/mm grating. Each sample was interrogated from 300-1800 cm-1 at 50% power with 20s integration time.

Molecular Docking

The docking was performed using the AutoDock Vina (Trott and Olson, 2010) plugin in UCSF Chimera (Pettersen et al., 2004). Chain A from PDB 1R4I was used, with residues 594 to 629 (human sequence numbering) removed to simulate unbinding of the helical segment. Prior to docking, the structure was prepared by adding hydrogen atoms and assigning charges to proteins and ligands. UCSF Chimera was used to prepare the structure of protein and ligand for docking and to view the docking result. The maximum number of binding modes generated is nine. AutoDock Vina gives a docking score, which is meant to predict the binding affinity in kcal/mol. We further analyzed the molecular interaction for the highest-scored docked compounds using LigPlot (Wallace et al., 1995) software.

Statistical Analysis

The luciferase values were summarized with mean and standard deviation. For comparisons between two groups, the luciferase values were log-transformed to meet the normality assumptions, followed by paired t-test. The p-values were corrected for multiplicity by Holm's approach when there were two or more comparisons. Because the study was designed as an early-stage and exploratory development, the p-values should be interpreted as descriptive.

Downloaded from molpharm.aspetjournals.org at ASPET Journals on July 7, 2023

Molecular Pharmacology Fast Forward. Published on January 31, 2023 as DOI: 10.1124/molpharm.122.000589
This article has not been copyedited and formatted. The final version may differ from this version.

Results

KCI807 does not bind within the NTD of AR

We have previously shown that the NTD of AR alone quantitatively accounts for the functional interaction of AR with ELK1 (Patki et al., 2013; Rosati et al., 2016). **Figure 1A** shows a schematic of the ELK1-interacting segments within the domain structure of AR. Within the NTD, the ELK1 binding segments in AR were previously mapped to amino acids 358-457 and 514-557 (Soave et al., 2022) **(Figure 1A).** To test whether KCI807 inhibited coactivation of ELK1 by AR by binding to a site within the NTD of AR, we used AR-negative recombinant HeLa cells (HeLa-HLR) harboring a TATA-dependent basal promoter-luciferase reporter *(GAL4-TATA-Luc)* and stably expressing a fusion protein in which the DNA binding domain of ELK1 was replaced by the Gal4 DNA binding domain. In this system, coactivation of ELK1 by AR may be monitored by measuring elevated luciferase activity in response to ectopic expression of full-length AR or deletion mutants of full-length AR, the NTD of AR or AR-V7. In the case of full-length AR and deletion mutants thereof, the transfected cells were treated with testosterone to enable entry of AR into the nucleus. Where necessary, western blotting was used to monitor expression of the AR constructs.

We first tested whether either ELK1-binding NTD segment within the full-length AR is required for the ability of KCI807 to inhibit coactivation of ELK1 by AR. To this end, we used deletion constructs of full-length AR in which either one of the two ELK1 binding segments in

Downloaded from molpharm.aspetjournals.org at ASPET Journals on July 7, 2023

Molecular Pharmacology Fast Forward. Published on January 31, 2023 as DOI: 10.1124/molpharm.122.000589
This article has not been copyedited and formatted. The final version may differ from this version.

the NTD (358-459 or 514-557) was deleted. When each mutant was expressed in HeLa-HLR cells, there was partial testosterone-dependent coactivation of ELK1, although deleting both motifs resulted in virtual loss of the AR-ELK1 interaction **(Figure 1B)**. We then examined the ability of KCI807 to inhibit residual ELK1-dependent promoter activation by AR in which either one of the ELK1 binding NTD segments was deleted. Neither deletion affected sensitivity of the ELK1-AR interaction to KCI807 **(Figure 1C)**, indicating that KCI807 did not bind to either site of interaction with ELK1 within the NTD in full-length AR.

We then tested whether the association of the AR NTD alone with ELK1 was inhibited by KCI807, possibly by the compound binding elsewhere within the NTD. For this purpose, we transfected HeLa-HLR cells with either an NTD-VP16 fusion protein (two-hybrid assay) or the isolated NTD (residues 1-557), which has intrinsic transcriptional activity. As seen in **Figure 1D,** coactivation of ELK1 by the VP16-NTD fusion protein was unaffected by KCI807. KCI807 was also unable to inhibit coactivation of ELK1 by the isolated NTD **(Figure 1E)**.

In contrast to the NTD, when HeLa-HLR cells were transfected with the AR-V7 variant that only includes the NTD and the DBD (residues 1-628), coactivation of ELK1 was inhibited by KCI807 **(Figure 1F)**. The results suggest that KCI807 may not bind within the NTD but rather, in the DBD.

Deletions and mutations within a DBD peptide motif flanking the NTD of AR disrupt interaction of ELK1 with AR and sensitivity to KCI807

As the preceding results indicate that the DBD rather than the NTD of AR may directly associate with KCI807, we used a mutagenesis approach to examine a possible role for any part of the DBD in mediating the effect of KCI807.

Downloaded from molpharm.aspetjournals.org at ASPET Journals on July 7, 2023

Molecular Pharmacology Fast Forward. Published on January 31, 2023 as DOI: 10.1124/molpharm.122.000589
This article has not been copyedited and formatted. The final version may differ from this version.

A series of consecutive, overlapping 10-amino acid deletions were made within the DBD in full length AR. These constructs were tested alongside wild type AR for their ability to coactivate ELK1 in a testosterone-dependent manner in HeLa-HLR cells **(Figure 2)**. Expression of the AR constructs was confirmed by western blot using antibody to AR **(Figure 2)**. Deletions spanning amino acids 558-594 within the DBD of AR all resulted in a substantial decrease in coactivation of ELK1 by AR **(Figure 2).** Deletions within the DBD downstream of amino acid 594 did not substantially affect coactivation of ELK1 by AR **(Figure 2).** As all of the deletion constructs showed at least residual co-activation of ELK1, we tested sensitivity of this co-activation to KCI807 in the inhibitor dose range of 1.25-10 μM. As seen in **Figure 3,** deletions spanning amino acids 558-594 all partially or fully decreased sensitivity of AR to KCI807, whereas deletions downstream of this region (amino acids 595-613) did not affect sensitivity of AR to KCI807.

To further investigate the apparent role of the peptide segment 558-594 in mediating the inhibitory effect of KCI807, we made several point mutations within this region, specifically I562A, H571A, T576A, C580A, and F583A **(Figure 4A)**. The mutant proteins all showed comparable expression, as seen from the western blot (**Figure 4B**). The point mutations variably affected the ability of AR to co-activate ELK1 **(Figure 4B)**. Notably though, the mutations I562A, C580A, and F583A resulted in reduced sensitivity to KCI807 **(Figure 4C).**

The above results functionally map the KCI807 binding site to within the peptide motif 558-594 in the DBD of AR.

KCI807 binds within the DNA binding domain of AR and blocks binding of an NTD polypeptide to ELK1

Downloaded from molpharm.aspetjournals.org at ASPET Journals on July 7, 2023

Molecular Pharmacology Fast Forward. Published on January 31, 2023 as DOI: 10.1124/molpharm.122.000589
This article has not been copyedited and formatted. The final version may differ from this version.

To further test the putative binding site for KCI807 within AR, we performed a GST-pulldown assay using purified His-tagged ELK1 and two purified GST-tagged AR polypeptide fragments. One AR fragment consisted of amino acids 334-566, which contained within it the ELK1 interacting NTD segments but did not fully encapsulate the mapped KCI807 binding site. The other fragment consisted of amino acids 328-631, which included the mapped KCI807 binding site and downstream DBD sequence **(Figure 5).** The 334-566 fragment was capable of binding ELK1 both in the absence and in the presence of KCI807. However, the 328-631 fragment bound ELK1 in the absence of KCI807 but was unable to bind ELK1 in the presence of KCI807 **(Figure 5).** This data offers biochemical validation that KCI807's binding site lies within the DBD.

Binding of KCI807 to the AR DBD induces Raman spectral changes indicative of a protein conformational change

We applied Raman spectroscopy as an independent method of examining the interaction of KCI807 with the DBD of AR. This method was chosen because of the higher sensitivity of Raman spectroscopy to small molecule-induced changes in protein conformation compared with most other types of direct binding assays. A KCI807 concentration of 2 μM was chosen in this experiment to ensure optimal binding of the compound to the AR DBD as this was in reasonable excess of the Kd value of $7x10^{-8}$ M previously determined for the binding of KCI807 to AR (Rosati et al., 2018). A commercially available purified rat AR polypeptide was used in equimolar ratio. As this rat AR polypeptide has a sequence that is identical to the sequence of the human AR DBD plus flanking sequences that have no similarity to any human AR sequence, it was used in lieu of a human AR DBD for the purpose of this experiment. The concentration of

Downloaded from molpharm.aspetjournals.org at ASPET Journals on July 7, 2023

Molecular Pharmacology Fast Forward. Published on January 31, 2023 as DOI: 10.1124/molpharm.122.000589
This article has not been copyedited and formatted. The final version may differ from this version.

KCI807 was too low to detect the Raman spectrum of the small molecule when compared with that of the vehicle (DMSO) control **(Figure 6A)**. When mixed with the AR DBD polypeptide, KCI807 induced several unique spectral features compared with the vehicle control as noted by the arrows in **Figure 6B**. Each of the changes represents aspects of the binding of KCI807. In particular, the changes in the region 1400 to 1450 are a classical reflection of considerable conformational change in a protein.

Location of the putative KCI807 binding site within the crystal structure of the AR DBD and molecular docking

The crystal structure of the AR DBD in a dimeric complex with its cognate DNA cis-element has been elucidated (Shaffer et al., 2004). As KCI807 does not interfere with the binding of AR to DNA (Rosati et al., 2018), we examined this crystal structure for a possible binding pocket for KCI807, comprising the putative KCI807 binding motif (residues 558-594) identified above. We used the amino acid residue numbering for human AR (Accession number NM_000044.6). Indeed, the crystal structure did reveal a pocket, rather precisely encompassed by residues 558-594 adjacent to the NTD but obscured by an alpha helix formed by residues 613-626 from the carboxy-terminal end of the DBD **(Figure 7A)**. This pocket lies outside the DNA binding surface formed by the zinc finger structure of the DBD **(Figure 7A)**. The three amino acid residues I562, C580, and F583, which were required for the integrity of the putative binding pocket based on the functional analysis above, line this cleft.

We next evaluated the potential for structure-specific docking of KCI807 within its putative binding pocket (amino acids 558-594) by *in silico* docking analysis. As the size of the putative binding pocket would obviously not accommodate analogs of KCI807 with bulky side

Downloaded from molpharm.aspetjournals.org at ASPET Journals on July 7, 2023

Molecular Pharmacology Fast Forward. Published on January 31, 2023 as DOI: 10.1124/molpharm.122.000589
This article has not been copyedited and formatted. The final version may differ from this version.

chains, we used previously published data (Rosati et al., 2018) on structure-activity relationships (SAR) obtained for closely structurally related KCI807 analogs of similar size. Accordingly, we generated an optimal docking model for KCI807 and then used this model to compare the docking scores for KCI807 with those obtained for three of its analogs. The analogs were: 1. 5,7,3',4'-tetrahydroxyflavone, which has similar activity as KCI807, indicating that the extra hydroxyl groups on C7 and C4' do not influence activity; 2. An isomer of this compound with an isoflavone scaffold rather than a flavone scaffold (5,7,3',4'-tetrahydroxy-isoflavone), which has no activity; and 3. A second isomer of the compound with an flavonone scaffold (5,7,3',4'-tetrahydroxy-flavonone) that has a 5-10 fold decreased activity compared with KCI807.

Figure 7B shows the DBD structure with the carboxy-terminal alpha helical segment removed to reveal the putative KCI807 binding pocket; the most energetically favorable docking mode for KCI807 is shown within this pocket. The size of the pocket is compatible with the size of the small molecule occupying it (molecular weight = 254 g/mol). KCI807 gave a docking score of -7.2 kcal/mol, which is a reasonable value for the measured Kd value of 70 nM for KCI807 as compared with a reported docking score of -7.3 kcal/mol for the binding of tamoxifen to the estrogen receptor (Xie et al., 2007) with a reported Kd of 5 nM (Coezy et al., 1982). The three amino acid residues determined in the point mutagenesis experiments above to be crucial for full activity of KCI807 (I562, C580, and F583) account for the hydrophobic interactions of the B ring of KCI807 **(Figure 7B)**. Additionally, T558 was further removed from the small molecule, consistent with retention of activity in the T558A mutant noted above. The 5-OH group in the A ring of KCI807, which was reported to be essential for activity in KCI807 (Rosati et al., 2018), forms a hydrogen bond with the backbone oxygen of H571. Note that this could be retained in the H571A mutant. Curiously, the 3'-OH group on the B ring, which is required for

Downloaded from molpharm.aspetjournals.org at ASPET Journals on July 7, 2023

Molecular Pharmacology Fast Forward. Published on January 31, 2023 as DOI: 10.1124/molpharm.122.000589
This article has not been copyedited and formatted. The final version may differ from this version.

optimal activity of KCI807 (Rosati et al., 2018), does not show hydrogen bonding, suggesting that there could be additional interactions with AR that are not captured by this model.

Consistent with the previously published experimental activity data, additional hydroxyl groups at positions C7 and C4' did not considerably affect the docking score (-7.1 kcal/mol) **(Supplemental Figure 1),** although interestingly the tetrahydroxy derivative of KCI807 showed an inverted binding configuration for optimal binding. This binding mode was disrupted in the complex with the isoflavone isomer, which adopted a reverse conformation and gave a considerably more positive docking score of -6.3 kcal/mol, consistent with the absence of activity in the dose range tested **(Supplemental Figure 2)**. The docking score for the flavonone isomer was intermediate between the flavone and isoflavone isomers, with a value of -6.9 kcal/mol, consistent with its observed reduced activity **(Supplemental Figure 3)**.

The *in silico* docking model for KCI807 is thus generally consistent with the binding affinity of KCI807 for AR and with relevant SAR data and mutagenesis data for the inhibitory action of KCI807 on coactivation of ELK1 by AR.

Downloaded from molpharm.aspetjournals.org at ASPET Journals on July 7, 2023

Molecular Pharmacology Fast Forward. Published on January 31, 2023 as DOI: 10.1124/molpharm.122.000589
This article has not been copyedited and formatted. The final version may differ from this version.

Discussion

The inability of KCI807 to inhibit the residual functional association of AR with ELK1 in deletion mutants of AR in which either one of the two ELK1 binding segments in the NTD was deleted indicated that the mechanism of action of KCI807 is not through direct competition with ELK1 for binding to the NTD. The insensitivity to KCI807 of the association of the isolated AR NTD to ELK1 was not only consistent with the above conclusion but further suggested that KCI807 may not bind to any region within the NTD. Further, the sensitivity of coactivation of ELK1 by AR-V7 to KCI807 suggested that the inhibitory activity of KCI807 may be mediated via the AR DBD, which lies immediately C-terminal to the NTD. Small internal deletions within the AR DBD, as well as point mutations, helped to map a polypeptide segment (residues 558-594) adjacent to the DBD whose structural integrity was not only necessary for optimal association of ELK1 with the NTD, but which was also necessary for the inhibitory effect of KCI807 on the association of ELK1 with the AR NTD. The requirement for the AR DBD for KCI807 to inhibit association of ELK1 with its binding region in the NTD of AR was directly confirmed using a GST pulldown assay. Raman spectroscopy not only provided additional direct evidence for the binding of KCI807 to the AR DBD, but further showed that a considerable conformational change was induced in the protein upon binding of the small molecule. Examination of the three-dimensional structure of a dimeric complex of the AR DBD with its cognate DNA element revealed folding of the KCI807 interacting segment in the DBD into a

Downloaded from molpharm.aspetjournals.org at ASPET Journals on July 7, 2023

Molecular Pharmacology Fast Forward. Published on January 31, 2023 as DOI: 10.1124/molpharm.122.000589
This article has not been copyedited and formatted. The final version may differ from this version.

potential binding pocket with the appropriate dimensions to accommodate KCI807. This pocket was outside the DNA binding surface of the DBD, consistent with previous observations that KCI807 did not interfere with androgen response element (ARE)-driven promoter activation by AR. The results of *in silico* docking studies of this putative binding pocket, using the known crystal structure of the DBD, gave a binding free energy similar to that for the binding of tamoxifen, a hydrophobic small molecule drug, to the hormone binding pocket of the estrogen receptor (ER) (Xie et al., 2007). In our model, amino acid residues I562, C580, and F583 shown by point mutagenesis in this study to be required for the binding of KCI807 were engaged in the hydrophobic binding interactions. Further, the model showed establishment of a hydrogen bond with the essential 5-OH group of KCI807, while suggesting that hydrogen bonding of the 3'-OH group required for optimal activity of KCI807 may occur in a more dynamic context. Finally, the docking scores for KCI807 and scaffold isomers of tetrahydroxy derivatives of KCI807 gave a pattern that corresponded to the previously published activity pattern of these compounds (Rosati et al., 2018).

Taken together, the results of this study lead to the conclusion that KCI807 must bind to the DBD of AR and induce a localized conformational change that would impinge on the NTD to block the binding of ELK1, without disrupting the ability of the DBD to bind to DNA. Although the extensive deletional and point mutagenesis studies implicate a segment of about 37 amino acids adjacent to the NTD in forming the KCI807 binding pocket, the exact nature of the conformational changes resulting from the binding of KCI807 could only be determined in the future through direct and high-resolution structural studies. Still, as a general mechanism, it may be expected that upon KCI807 binding, one or more downstream elements in the DBD may be displaced or mobilized to interact with the NTD, disrupting ELK1 binding. For example,

Downloaded from molpharm.aspetjournals.org at ASPET Journals on July 7, 2023

Molecular Pharmacology Fast Forward. Published on January 31, 2023 as DOI: 10.1124/molpharm.122.000589
This article has not been copyedited and formatted. The final version may differ from this version.

displacement of the carboxyl-terminal alpha helical segment of the DBD which buttresses the putative KCI807 binding pocket may not affect the site of DNA binding while mobilizing a segment of the DBD to interact with the NTD.

In the context of the above mechanism, it is relevant to note that domain interactions are known to occur within the AR polypeptide, with considerable functional effects. It has been reported that the binding of DNA to the AR DBD causes conformational changes in the NTD, indicated by changes in tryptophan fluorescence and protease sensitivity; conversely, the NTD modulated the affinity of binding of the DBD to DNA (Brodie and McEwan, 2005). Indeed, mutagenesis studies have revealed that the NTD also critically modulates the LBD by associating with AF2 in the LBD to stabilize helix 12 in the LBD, resulting in a decrease in the dissociation rate of dihydrotestosterone (He et al., 1999). It should be unsurprising then that small conformational changes in the DBD would affect protein interactions of the NTD as suggested here by our studies.

Despite similarities in structural organization and functions among steroid receptors, there is no amino acid sequence conservation among the NTDs of these proteins (Papageorgiou et al., 2021). The entire NTD of AR is characteristically unstructured overall, with a general pattern of stretches of flexible structures of variable lengths highly enriched in small residues (G, A), polar residues (N, Q, S, T) or proline (P) between shorter sequences comprising mostly large hydrophobic residues and charged residues that are known to contribute to more rigid structural elements (McEwan et al., 2007). It has been proposed (McEwan et al., 2007) that this feature of the NTD allows for the availability of peptide motifs as well as adequate flexibility for specific protein-protein interactions with many coregulator proteins that are known to associate with the NTD of AR (Lavery and McEwan, 2008; Markus et al., 2002; McEwan and Kumar, 2015).

Downloaded from molpharm.aspetjournals.org at ASPET Journals on July 7, 2023

Molecular Pharmacology Fast Forward. Published on January 31, 2023 as DOI: 10.1124/molpharm.122.000589
This article has not been copyedited and formatted. The final version may differ from this version.

However, the NTD may not have adequate structural integrity to form high affinity binding pockets for highly specific associations of small molecules. Moreover, given the relatively large protein segments in the NTD that are required for the association of AR with ELK1 (Soave et al., 2022), a small molecule may not be able to quantitatively block ELK1 binding to AR by direct competition for binding to the NTD. Indeed, structural studies have shown that the coactivator binding site (AF2) in the LBD of the estrogen receptor presents a relatively large area with multiple binding elements, limiting the efficacy of coactivator binding inhibitors of a relatively small size (Sun et al., 2011). The foregoing considerations, combined with the model for the action of KCI807 developed in this study, may have implications in current efforts to develop small molecule drugs that block other critical protein interactions with the NTD of AR (Monaghan and McEwan, 2016). In such efforts, it may be a practical approach to seek small molecules that would bind specifically to a well-structured domain in the AR and modulate domain interactions that would interfere with the function of the NTD.

Given the major problem of resistance of advanced AR-dependent PCa to hormone-based therapies, including the emergence of AR splice variants, the importance of developing small molecule drugs that target AR domains outside the LBD cannot be understated. Accordingly, there are ongoing efforts to develop drugs that inhibit critical protein-protein interactions of the NTD and DBD and also dimerization or DNA binding of the DBD (Li et al., 2014; Monaghan and McEwan, 2016; Monaghan et al., 2022; Radaeva et al., 2021). In this regard, KCI807-based drugs potentially offer an additional advantage in that they would inhibit growth of advanced PCa by narrowly inhibiting the AR-ELK1 axis, without also affecting broader AR functions such as coregulator binding and DNA binding that may be needed for AR signaling in a variety of differentiated normal tissues (Rosati et al., 2018). Identification in this study of a putative

Downloaded from molpharm.aspetjournals.org at ASPET Journals on July 7, 2023

Molecular Pharmacology Fast Forward. Published on January 31, 2023 as DOI: 10.1124/molpharm.122.000589
This article has not been copyedited and formatted. The final version may differ from this version.

binding pocket for KCI807 within the DBD of AR and the implication that DBD-NTD interactions mediate the inhibitory effect of KCI807 on ELK1 binding has set the stage for high-resolution structural studies, such as X-ray crystallography and NMR, to elucidate the precise nature of these interactions. The studies should enable rational design of next generation molecules that target the AR-ELK1 complex for therapeutic intervention in advanced prostate cancer that is resistant to testosterone suppression.

Downloaded from molpharm.aspetjournals.org at ASPET Journals on July 7, 2023

Molecular Pharmacology Fast Forward. Published on January 31, 2023 as DOI: 10.1124/molpharm.122.000589
This article has not been copyedited and formatted. The final version may differ from this version.

Acknowledgements

The authors are grateful to Ms. Jean Guerin for administrative assistance and to Ms. Janice Saxton for technical assistance.

Downloaded from molpharm.aspetjournals.org at ASPET Journals on July 7, 2023

Molecular Pharmacology Fast Forward. Published on January 31, 2023 as DOI: 10.1124/molpharm.122.000589
This article has not been copyedited and formatted. The final version may differ from this version.

Authorship Contributions

Participated in research design: Ratnam M, Soave C, Shaw P, Ducker C, Auner G, Islam N, Dickson A

Conducted experiments: Soave C, Ducker C, Huang Y, Yurgelevic S

Contributed new reagents or analytic tools: Islam N, Auner G

Performed data analysis: Ratnam M, Soave C, Ducker C, Nicely N, Shaw P, Kim S, Pardy L, Auner G, Islam N, Dickson A

Wrote or contributed to the writing of the manuscript: Ratnam M, Soave C, Ducker C, Nicely N, Kim S, Shaw P, Auner G, Islam N, Dickson A

Downloaded from molpharm.aspetjournals.org at ASPET Journals on July 7, 2023

Molecular Pharmacology Fast Forward. Published on January 31, 2023 as DOI: 10.1124/molpharm.122.000589
This article has not been copyedited and formatted. The final version may differ from this version.

References

Bevan CL, Hoare S, Claessens F, Heery DM and Parker MG (1999) The AF1 and AF2 domains of the androgen receptor interact with distinct regions of SRC1. *Mol Cell Biol* **19**(12): 8383-8392.

Brodie J and McEwan IJ (2005) Intra-domain communication between the N-terminal and DNA-binding domains of the androgen receptor: modulation of androgen response element DNA binding. *J Mol Endocrinol* **34**(3): 603-615.

Christiaens V, Bevan CL, Callewaert L, Haelens A, Verrijdt G, Rombauts W and Claessens F (2002) Characterization of the two coactivator-interacting surfaces of the androgen receptor and their relative role in transcriptional control. *J Biol Chem* **277**(51): 49230-49237.

Coezy E, Borgna JL and Rochefort H (1982) Tamoxifen and metabolites in MCF7 cells: correlation between binding to estrogen receptor and inhibition of cell growth. *Cancer Res* **42**(1): 317-323.

Dunn MW and Kazer MW (2011) Prostate cancer overview. *Semin Oncol Nurs* **27**(4): 241-250.

Gille H, Sharrocks AD and Shaw PE (1992) Phosphorylation of transcription factor p62TCF by MAP kinase stimulates ternary complex formation at c-fos promoter. *Nature* **358**(6385): 414-417.

He B, Kemppainen JA, Voegel JJ, Gronemeyer H and Wilson EM (1999) Activation function 2 in the human androgen receptor ligand binding domain mediates interdomain communication with the NH(2)-terminal domain. *J Biol Chem* **274**(52): 37219-37225.

Henzler C, Li Y, Yang R, McBride T, Ho Y, Sprenger C, Liu G, Coleman I, Lakely B, Li R, Ma S, Landman SR, Kumar V, Hwang TH, Raj GV, Higano CS, Morrissey C, Nelson PS, Plymate SR

Downloaded from molpharm.aspetjournals.org at ASPET Journals on July 7, 2023

Molecular Pharmacology Fast Forward. Published on January 31, 2023 as DOI: 10.1124/molpharm.122.000589
This article has not been copyedited and formatted. The final version may differ from this version.

and Dehm SM (2016) Truncation and constitutive activation of the androgen receptor by diverse genomic rearrangements in prostate cancer. *Nature Communications* **7**(1): 13668.

Hu R, Lu C, Mostaghel EA, Yegnasubramanian S, Gurel M, Tannahill C, Edwards J, Isaacs WB, Nelson PS, Bluemn E, Plymate SR and Luo J (2012) Distinct transcriptional programs mediated by the ligand-dependent full-length androgen receptor and its splice variants in castration-resistant prostate cancer. *Cancer Res* **72**(14): 3457-3462.

Koryakina Y, Ta HQ and Gioeli D (2014) Androgen receptor phosphorylation: biological context and functional consequences. *Endocr Relat Cancer* **21**(4): T131-145.

Kounatidou E, Nakjang S, McCracken SRC, Dehm SM, Robson CN, Jones D and Gaughan L (2019) A novel CRISPR-engineered prostate cancer cell line defines the AR-V transcriptome and identifies PARP inhibitor sensitivities. *Nucleic Acids Res* **47**(11): 5634-5647.

Lavery DN and McEwan IJ (2008) Functional characterization of the native NH2-terminal transactivation domain of the human androgen receptor: binding kinetics for interactions with TFIIF and SRC-1a. *Biochemistry* **47**(11): 3352-3359.

Li H, Ban F, Dalal K, Leblanc E, Frewin K, Ma D, Adomat H, Rennie PS and Cherkasov A (2014) Discovery of small-molecule inhibitors selectively targeting the DNA-binding domain of the human androgen receptor. *J Med Chem* **57**(15): 6458-6467.

Li Y, Chan SC, Brand LJ, Hwang TH, Silverstein KA and Dehm SM (2013) Androgen receptor splice variants mediate enzalutamide resistance in castration-resistant prostate cancer cell lines. *Cancer Res* **73**(2): 483-489.

Loblaw DA, Virgo KS, Nam R, Somerfield MR, Ben-Josef E, Mendelson DS, Middleton R, Sharp SA, Smith TJ, Talcott J, Taplin M, Vogelzang NJ, Wade JL, 3rd, Bennett CL and Scher HI (2007) Initial hormonal management of androgen-sensitive metastatic, recurrent, or progressive prostate cancer: 2006 update of an American Society of Clinical Oncology practice guideline. *J Clin Oncol* **25**(12): 1596-1605.

Downloaded from molpharm.aspetjournals.org at ASPET Journals on July 7, 2023

Molecular Pharmacology Fast Forward. Published on January 31, 2023 as DOI: 10.1124/molpharm.122.000589
This article has not been copyedited and formatted. The final version may differ from this version.

MacLean HE, Warne GL and Zajac JD (1997) Localization of functional domains in the androgen receptor. *J Steroid Biochem Mol Biol* **62**(4): 233-242.

Markus SM, Taneja SS, Logan SK, Li W, Ha S, Hittelman AB, Rogatsky I and Garabedian MJ (2002) Identification and characterization of ART-27, a novel coactivator for the androgen receptor N terminus. *Mol Biol Cell* **13**(2): 670-682.

McEwan IJ and Kumar R (2015) *Nuclear Receptors: From Structure to the Clinic*. Springer International Publishing.

McEwan IJ, Lavery D, Fischer K and Watt K (2007) Natural disordered sequences in the amino terminal domain of nuclear receptors: lessons from the androgen and glucocorticoid receptors. *Nucl Recept Signal* **5**: e001.

Monaghan AE and McEwan IJ (2016) A sting in the tail: the N-terminal domain of the androgen receptor as a drug target. *Asian J Androl* **18**(5): 687-694.

Monaghan AE, Porter A, Hunter I, Morrison A, McElroy SP and McEwan IJ (2022) Development of a High-Throughput Screening Assay for Small-Molecule Inhibitors of Androgen Receptor Splice Variants. *Assay Drug Dev Technol* **20**(3): 111-124.

Nyquist MD, Li Y, Hwang TH, Manlove LS, Vessella RL, Silverstein KAT, Voytas DF and Dehm SM (2013) TALEN-engineered AR gene rearrangements reveal endocrine uncoupling of androgen receptor in prostate cancer. *Proceedings of the National Academy of Sciences* **110**(43): 17492-17497.

Papageorgiou L, Shalzi L, Efthimiadou A, Bacopoulou F, Chrousos GP, Eliopoulos E and Vlachakis D (2021) Conserved functional motifs of the nuclear receptor superfamily as potential pharmacological targets. *Int J Epigen* **1**(2): 3.

Pardy L, Rosati R, Soave C, Huang Y, Kim S and Ratnam M (2020) The ternary complex factor protein ELK1 is an independent prognosticator of disease recurrence in prostate cancer. *Prostate* **80**(2): 198-208.

Downloaded from molpharm.aspetjournals.org at ASPET Journals on July 7, 2023

Molecular Pharmacology Fast Forward. Published on January 31, 2023 as DOI: 10.1124/molpharm.122.000589
This article has not been copyedited and formatted. The final version may differ from this version.

Patki M, Chari V, Sivakumaran S, Gonit M, Trumbly R and Ratnam M (2013) The ETS domain transcription factor ELK1 directs a critical component of growth signaling by the androgen receptor in prostate cancer cells. *J Biol Chem* **288**(16): 11047-11065.

Pettersen EF, Goddard TD, Huang CC, Couch GS, Greenblatt DM, Meng EC and Ferrin TE (2004) UCSF Chimera--a visualization system for exploratory research and analysis. *J Comput Chem* **25**(13): 1605-1612.

Radaeva M, Ban F, Zhang F, LeBlanc E, Lallous N, Rennie PS, Gleave ME and Cherkasov A (2021) Development of Novel Inhibitors Targeting the D-Box of the DNA Binding Domain of Androgen Receptor. *Int J Mol Sci* **22**(5).

Rosati R, Patki M, Chari V, Dakshnamurthy S, McFall T, Saxton J, Kidder BL, Shaw PE and Ratnam M (2016) The Amino-terminal Domain of the Androgen Receptor Co-opts Extracellular Signal-regulated Kinase (ERK) Docking Sites in ELK1 Protein to Induce Sustained Gene Activation That Supports Prostate Cancer Cell Growth. *J Biol Chem* **291**(50): 25983-25998.

Rosati R, Polin L, Ducker C, Li J, Bao X, Selvakumar D, Kim S, Xhabija B, Larsen M, McFall T, Huang Y, Kidder BL, Fribley A, Saxton J, Kakuta H, Shaw P and Ratnam M (2018) Strategy for Tumor-Selective Disruption of Androgen Receptor Function in the Spectrum of Prostate Cancer. *Clin Cancer Res* **24**(24): 6509-6522.

Shaffer PL, Jivan A, Dollins DE, Claessens F and Gewirth DT (2004) Structural basis of androgen receptor binding to selective androgen response elements. *Proc Natl Acad Sci U S A* **101**(14): 4758-4763.

Shaw PE and Saxton J (2003) Ternary complex factors: prime nuclear targets for mitogen-activated protein kinases. *Int J Biochem Cell Biol* **35**(8): 1210-1226.

Sun A, Moore TW, Gunther JR, Kim MS, Rhoden E, Du Y, Fu H, Snyder JP and Katzenellenbogen JA (2011) Discovering small-molecule estrogen receptor α/coactivator binding inhibitors: high-throughput screening, ligand development, and models for enhanced potency. *ChemMedChem* **6**(4): 654-666.

Downloaded from molpharm.aspetjournals.org at ASPET Journals on July 7, 2023

Molecular Pharmacology Fast Forward. Published on January 31, 2023 as DOI: 10.1124/molpharm.122.000589
This article has not been copyedited and formatted. The final version may differ from this version.

Sun S, Sprenger CC, Vessella RL, Haugk K, Soriano K, Mostaghel EA, Page ST, Coleman IM, Nguyen HM, Sun H, Nelson PS and Plymate SR (2010) Castration resistance in human prostate cancer is conferred by a frequently occurring androgen receptor splice variant. *J Clin Invest* **120**(8): 2715-2730.

Teo MY, Rathkopf DE and Kantoff P (2019) Treatment of Advanced Prostate Cancer. *Annu Rev Med* **70**: 479-499.

Trott O and Olson AJ (2010) AutoDock Vina: improving the speed and accuracy of docking with a new scoring function, efficient optimization, and multithreading. *J Comput Chem* **31**(2): 455-461.

Visakorpi T, Hyytinen E, Koivisto P, Tanner M, Keinänen R, Palmberg C, Palotie A, Tammela T, Isola J and Kallioniemi OP (1995) In vivo amplification of the androgen receptor gene and progression of human prostate cancer. *Nat Genet* **9**(4): 401-406.

Wallace AC, Laskowski RA and Thornton JM (1995) LIGPLOT: a program to generate schematic diagrams of protein-ligand interactions. *Protein Eng* **8**(2): 127-134.

Xie L, Wang J and Bourne PE (2007) In silico elucidation of the molecular mechanism defining the adverse effect of selective estrogen receptor modulators. *PLoS Comput Biol* **3**(11): e217.

Yu J, Yu J, Mani RS, Cao Q, Brenner CJ, Cao X, Wang X, Wu L, Li J, Hu M, Gong Y, Cheng H, Laxman B, Vellaichamy A, Shankar S, Li Y, Dhanasekaran SM, Morey R, Barrette T, Lonigro RJ, Tomlins SA, Varambally S, Qin ZS and Chinnaiyan AM (2010) An integrated network of androgen receptor, polycomb, and TMPRSS2-ERG gene fusions in prostate cancer progression. *Cancer Cell* **17**(5): 443-454.

Zhang HM, Li L, Papadopoulou N, Hodgson G, Evans E, Galbraith M, Dear M, Vougier S, Saxton J and Shaw PE (2008) Mitogen-induced recruitment of ERK and MSK to SRE promoter complexes by ternary complex factor Elk-1. *Nucleic Acids Res* **36**(8): 2594-2607.

Downloaded from molpharm.aspetjournals.org at ASPET Journals on July 7, 2023

Molecular Pharmacology Fast Forward. Published on January 31, 2023 as DOI: 10.1124/molpharm.122.000589
This article has not been copyedited and formatted. The final version may differ from this version.

Footnotes:

This work was supported by the U.S. Department of Defense (Grant W81XWH-17-1-0242 to M.R. and Grant W81XWH-17-1-0243 to P.E.S.) and the National Institutes of Health (Grant 5T32CA009531-29 to C.S.). No author has an actual or perceived conflict of interest with the contents of this article.

Downloaded from molpharm.aspetjournals.org at ASPET Journals on July 7, 2023

Molecular Pharmacology Fast Forward. Published on January 31, 2023 as DOI: 10.1124/molpharm.122.000589
This article has not been copyedited and formatted. The final version may differ from this version.

Legends to Figures:

Fig. 1: Identification of the KCI807 binding domain of AR. A. Schematic representation showing the domain organization of AR, functional subdomains and the two ELK1-interacting segments. **B.** HeLa-HLR cells were transfected with an expression plasmid for wild type AR (100 ng, 150 ng and 200 ng DNA), a mutant AR construct with deletion of either one of the two ELK1-interacting segments in the NTD (residues 358-459 or 514-557) (100 ng DNA) or a mutant AR with a double deletion of the two ELK1-interacting segments in the NTD (residues 358-459 and 514-557) (100 ng DNA). Cells were harvested 48h after transfection and cell lysates were prepared from parallel wells for measurement of luciferase activity and western blotting. The western blots were probed with antibody against AR or GAPDH (loading control). The luciferase values from experimental triplicates are plotted; $*P = 0.0043$, $**P = 0.0043$. **C.** HeLa-HLR cells in the presence of testosterone (10 nM), were transfected with an expression plasmid (150 ng DNA) for either wild type AR or a mutant AR construct with deletion of either ELK1-interacting segment (residues 358-459 or 514-557). Cells were then treated with vehicle (DMSO) or KCI807. Cells were harvested 48h after transfection for preparation of cell lysates to measure luciferase activity. The luciferase values from experimental triplicates are plotted; $*P < 0.05$, $**P < 0.01$, $***P < 0.001$. **D.** HeLa-HLR cells were transfected with an expression plasmid (300 ng DNA) for a fusion protein of the AR NTD (residues 1-557) with VP16 (VP16-NTD).

Downloaded from molpharm.aspetjournals.org at ASPET Journals on July 7, 2023

Molecular Pharmacology Fast Forward. Published on January 31, 2023 as DOI: 10.1124/molpharm.122.000589
This article has not been copyedited and formatted. The final version may differ from this version.

Cells were then treated with vehicle (DMSO) or KCI807. Cells were harvested 48h after transfection for preparation of cell lysates to measure luciferase activity. The luciferase values from experimental triplicates are plotted. **E.** HeLa-HLR cells were transfected with an expression plasmid (400 ng DNA) for the AR NTD alone (residues 1-557). Cells were then treated with vehicle (DMSO) or KCI807. Cells were harvested 48h after transfection for preparation of cell lysates to measure luciferase activity. The luciferase values from experimental triplicates are plotted. **F.** HeLa-HLR cells were transfected with an expression plasmid (400 ng DNA) for AR-V7. Cells were then treated with vehicle (DMSO) or KCI807. Cells were harvested 48h after transfection for preparation of cell lysates to measure luciferase activity (Relative luciferase units for vehicle control = 5.28×10^6). The luciferase values from experimental triplicates are plotted; * $P = 0.00534$; ** $P = 0.0053$. Statistical significance was assessed using a paired t-test followed by the Holm's post-hoc correction (B, C, F).

Fig. 2: Effect of deleting peptide segments within a region of the DBD of AR flanking the NTD on the ability of AR to coactivate ELK1. HeLa-HLR cells were treated with either vehicle or testosterone (10 nM) and transfected individually with an expression plasmid (200 ng DNA) for wild type AR or mutants of AR with sequential deletions (overlapping or consecutive) within the DBD of AR (residues 558-568, 563-573, 568-578, 574-584, 580-590, 585-595, 595-604, 605-613). Cells were harvested 48h after transfection for preparation of cell lysates to measure luciferase activity (Relative luciferase units for wtAR with testosterone = 6.67×10^6) and for western blotting. Western blots were probed with antibody against AR or GAPDH (loading control). The luciferase values from experimental triplicates are plotted; * $P < 0.01$, ** P

Downloaded from molpharm.aspetjournals.org at ASPET Journals on July 7, 2023

Molecular Pharmacology Fast Forward. Published on January 31, 2023 as DOI: 10.1124/molpharm.122.000589
This article has not been copyedited and formatted. The final version may differ from this version.

< 0.001. Statistical significance was assessed using a paired t-test followed by the Holm's post-hoc correction.

Fig. 3: Effect of deletions within the DBD region flanking the NTD of AR on the sensitivity of residual ELK1 coactivation to KCI807. HeLa-HLR cells were treated with testosterone (10 nM) and transfected individually with expression plasmid (200 ng DNA) for wild type AR or mutants of AR with sequential deletions (overlapping or consecutive) within the DBD of AR (residues 558-568, 563-573, 568-578, 574-584, 580-590, 585-595, 595-604, 605-613). Cells were then treated with vehicle (DMSO) or KCI807. Cells were harvested 48h after transfection for preparation of cell lysates to measure luciferase activity. The luciferase values from experimental triplicates are plotted; $^{\#}P=0.0547$, $*P < 0.05$, $** P < 0.01$, $***P < 0.001$. Note: In the KCI807 sensitivity data presented in Figure 3, the luciferase values for the control for each AR construct (without KCI807) is normalized to a value of 100 percent. The relative abilities of the constructs to coactivate ELK1 in a testosterone-dependent manner are shown in Figure 2 and the actual luciferase activity units are indicated in the legend to Figure 2. Statistical significance was assessed using a paired t-test followed by the Holm's post-hoc correction.

Fig. 4: Effect of point mutations within the peptide segment 558-594 in the DBD of AR on ELK1 coactivation and sensitivity to KCI807. A. Amino acid sequence of the peptide 558-594 within the DBD of AR. Red font indicates amino acid residues that were mutated to alanine. **B.** HeLa-HLR cells were treated with either vehicle or testosterone (10 nM) and transfected individually with expression plasmids (200 ng DNA) for wild type AR or point mutants of AR (I562A, H571A, T576A, C580A and F583A). Cells were harvested 48h after transfection for

Downloaded from molpharm.aspetjournals.org at ASPET Journals on July 7, 2023

Molecular Pharmacology Fast Forward. Published on January 31, 2023 as DOI: 10.1124/molpharm.122.000589
This article has not been copyedited and formatted. The final version may differ from this version.

preparation of cell lysates to measure luciferase activity and western blotting. Western blots were probed with antibody against AR or GAPDH (loading control). The luciferase values from experimental triplicates are plotted; *$P < 0.01$, **$P < 0.001$, ***$P < 0.0001$. **C.** HeLa-HLR cells were treated with testosterone (10 nM) and transfected individually with expression plasmid (200 ng DNA) for wild type AR or point mutants of AR (I562A, H571A, T576A, C580A and F583A). Cells were then treated with vehicle (DMSO) or KCI807. Cells were harvested 48h after transfection for preparation of cell lysates to measure luciferase activity. The luciferase values from experimental triplicates are plotted;* *$P < 0.05$, ** $P < 0.01$, *** $P<0.001$*. Note: In the KCI807 sensitivity data presented in Figure 4C, the luciferase values for the control for each AR construct (without KCI807) is normalized to a value of 100 percent. The relative abilities of the constructs to coactivate ELK1 in a testosterone-dependent manner are shown in terms of the actual luciferase activity units in Figure 4B. Statistical significance was assessed using a paired t-test followed by the Holm's post-hoc correction (B, C).

Fig. 5: Localization of the KCI807 binding region in AR using a GST pulldown assay of ELK1 binding to AR polypeptides. Recombinant GST-tagged AR fragments were incubated with KCI807 (1μM) or vehicle (DMSO) before addition of ELK1-His. Proteins retained on glutathione sepharose beads after washing were identified by western blot using antibodies to probe for ELK1 (top left panel) and GST (bottom left panel). Schematics (right side) highlight regions of AR included in protein constructs, including the upstream and downstream ELK1 interaction segments (black and dark grey boxes, respectively) within the NTD and the putative KCI807 binding site (light grey) within the DBD.

Downloaded from molpharm.aspetjournals.org at ASPET Journals on July 7, 2023

Molecular Pharmacology Fast Forward. Published on January 31, 2023 as DOI: 10.1124/molpharm.122.000589
This article has not been copyedited and formatted. The final version may differ from this version.

Fig. 6: Raman spectral changes induced in the AR DBD by KCI807. A. Raman spectra of KCI807 (2 μM) in phosphate buffered saline compared with that of vehicle control (0.02 percent DMSO) the same buffer. **B.** Raman spectra of the AR DBD polypeptide (2 μM) combined with KCI807 (2 uM) in phosphate buffered saline compared with that of the AR DBD polypeptide (2 μM) combined with vehicle control (0.02 percent DMSO) in the same buffer.

Fig. 7: *In silico* analysis of the crystal structure of the AR DBD to identify a potential binding pocket for KCI807. A. The carboxy-terminal alpha helix of the DBD (residues 613-626) is shown in cartoon representation with the rest of the domain in surface representation. The surface is colored by the electrostatic potential using the "coulombic" function of UCSF Chimera, with negative charge in red and positive charge in blue. **B.** The highest scoring pose for KCI807 docked in the DBD pocket (right), the 2D structure of KCI807 (left), and a LigPlot showing hydrogen bonding interactions (dashed green line) and hydrophobic interactions (red starbursts). The amino acids are numbered according to the human AR sequence accession number NM_000044.6.

Downloaded from molpharm.aspetjournals.org at ASPET Journals on July 7, 2023

Molecular Pharmacology Fast Forward. Published on January 31, 2023 as DOI: 10.1124/molpharm.122.000589
This article has not been copyedited and formatted. The final version may differ from this version.

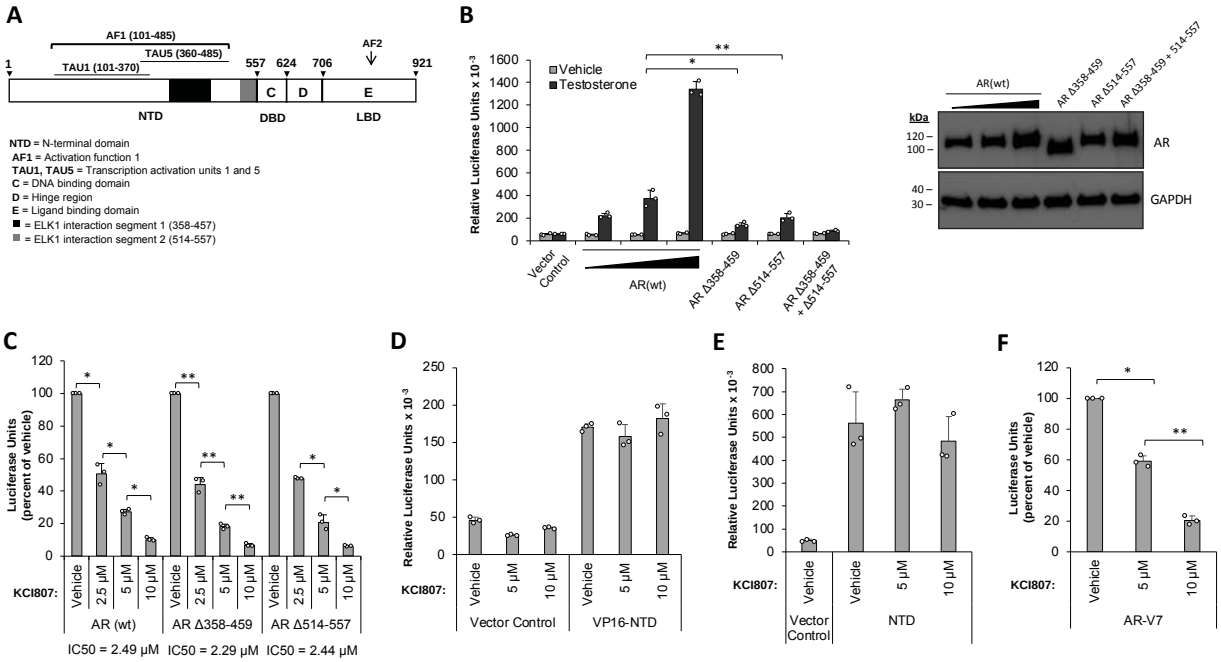

Figure 1

Downloaded from molpharm.aspetjournals.org at ASPET Journals on July 7, 2023

Molecular Pharmacology Fast Forward. Published on January 31, 2023 as DOI: 10.1124/molpharm.122.000589
This article has not been copyedited and formatted. The final version may differ from this version.

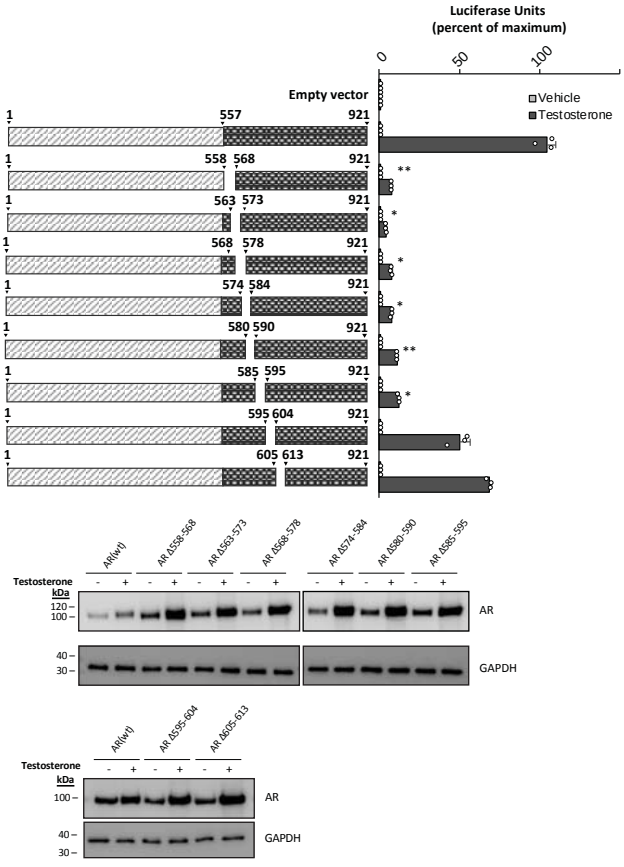

Figure 2

Downloaded from molpharm.aspetjournals.org at ASPET Journals on July 7, 2023

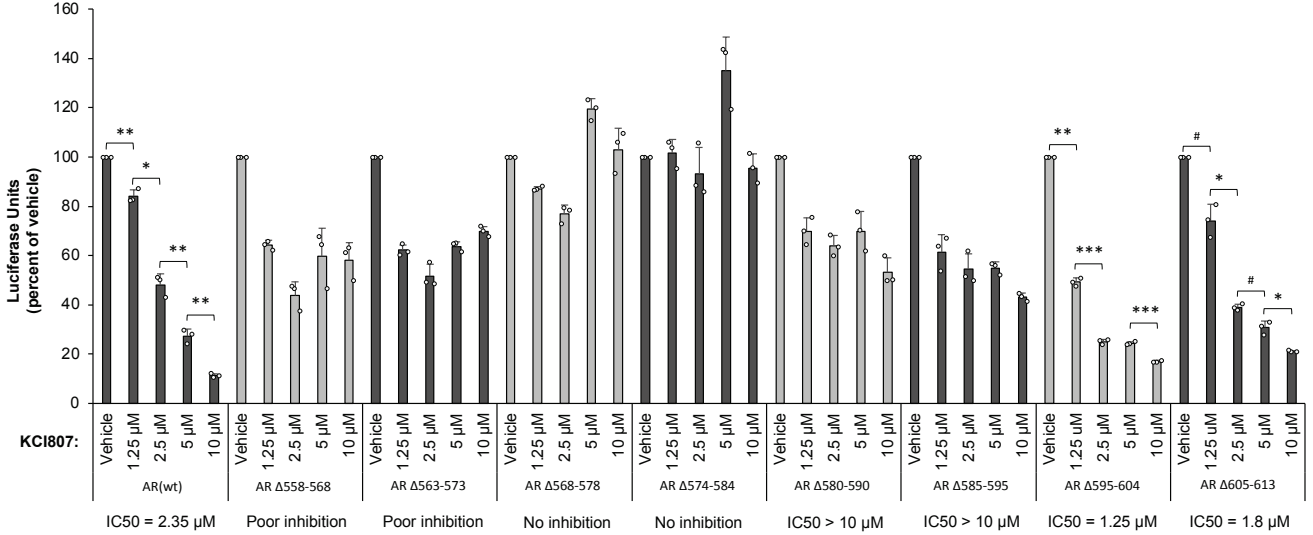
Luciferase Units
(percent of vehicle)
160
140
120
100
80
60
40
20
0
KCl807:
Vehicle
1.25 µM
2.5 µM
5 µM
10 µM
AR(wt)
AR Δ558-568
AR Δ563-573
AR Δ568-578
AR Δ574-584
AR Δ580-590
AR Δ585-595
AR Δ595-604
AR Δ605-613
IC50 = 2.35 µM
Poor inhibition
Poor inhibition
No inhibition
No inhibition
IC50 > 10 µM
IC50 > 10 µM
IC50 = 1.25 µM
IC50 = 1.8 µM

Figure 3

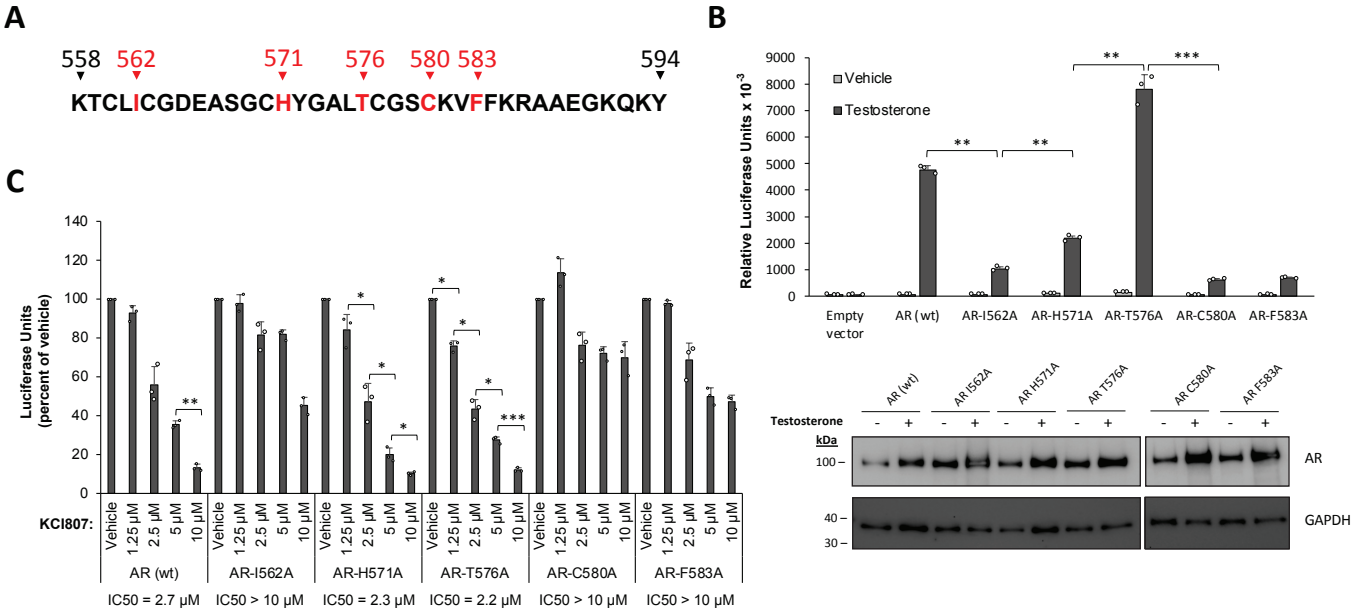
A
558
562
571
576
580
583
594
KTCLICGDEASGCHYGALTCGSCKVFFKRAAEGKQKY
B
Relative Luciferase Units x 10-3
Vehicle
Testosterone
Empty vector
AR (wt)
AR-I562A
AR-H571A
AR-T576A
AR-C580A
AR-F583A
Testosterone
kDa
100 –
40 –
30 –
AR
GAPDH
C
Luciferase Units (percent of vehicle)
KCI807:
Vehicle
1.25 µM
2.5 µM
5 µM
10 µM
AR (wt)
AR-I562A
AR-H571A
AR-T576A
AR-C580A
AR-F583A
IC50 = 2.7 µM
IC50 > 10 µM
IC50 = 2.3 µM
IC50 = 2.2 µM
IC50 > 10 µM
IC50 > 10 µM

Figure 4

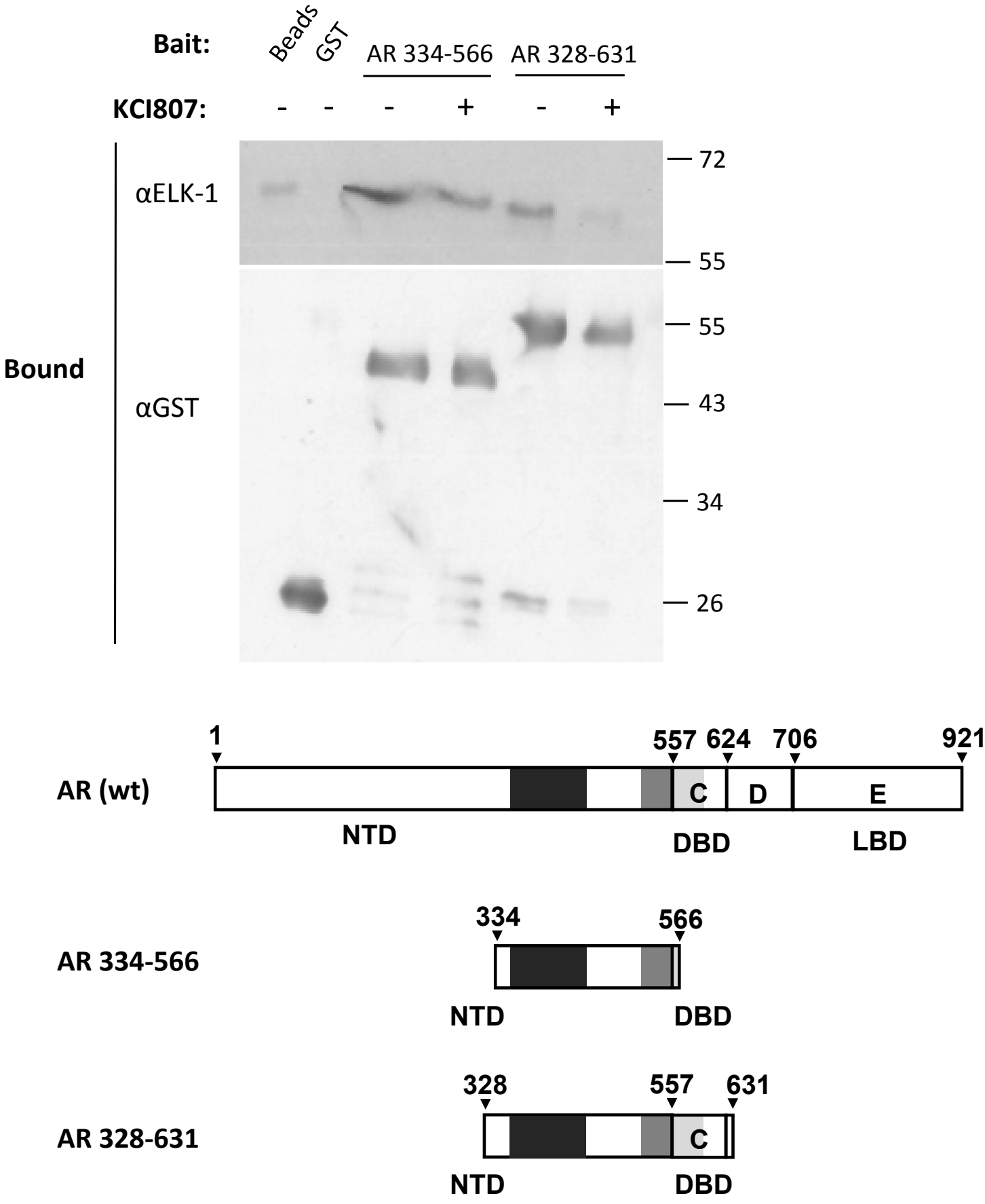
Bait:
Beads
GST
AR 334-566
AR 328-631
KCl807:
- - - + - +
Bound
αELK-1
αGST
72
55
55
43
34
26
AR (wt)
1
557
624
706
921
C
D
E
NTD
DBD
LBD
AR 334-566
334
566
NTD
DBD
AR 328-631
328
557
631
C
NTD
DBD

Figure 5

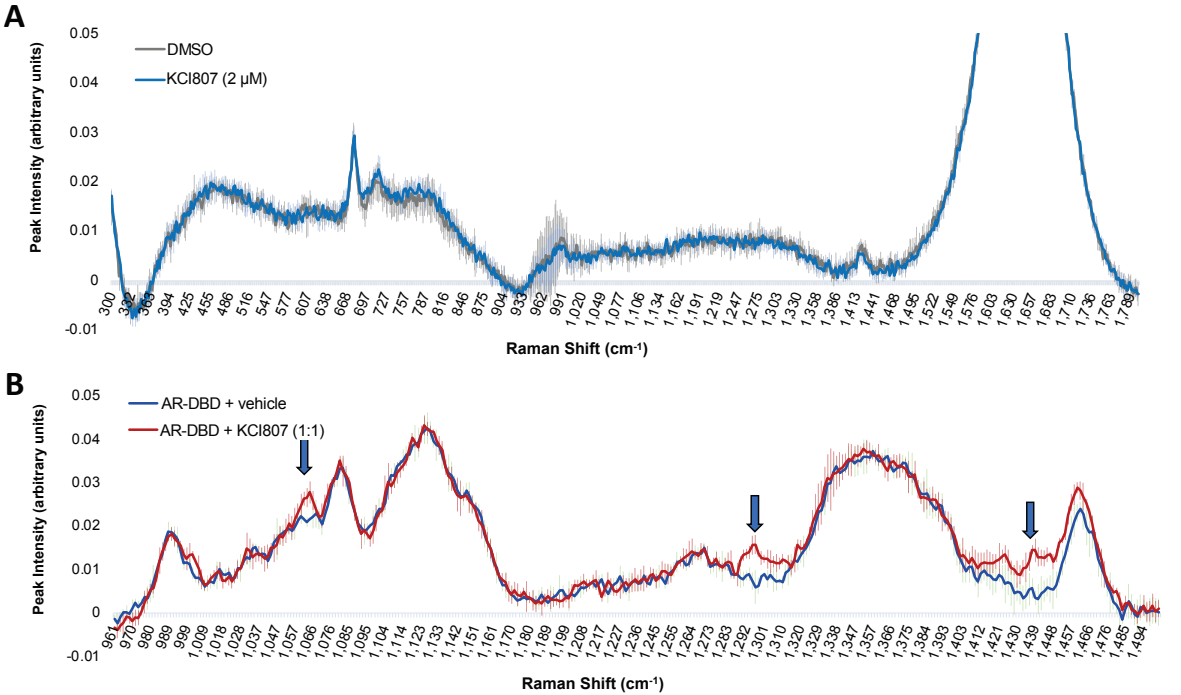
A
DMSO
KCl807 (2 μM)
Peak Intensity (arbitrary units)
Raman Shift (cm-1)
B
AR-DBD + vehicle
AR-DBD + KCl807 (1:1)
Peak Intensity (arbitrary units)
Raman Shift (cm-1)

Figure 6

Molecular Pharmacology Fast Forward. Published on January 31, 2023 as DOI: 10.1124/molpharm.122.000589
This article has not been copyedited and formatted. The final version may differ from this version.

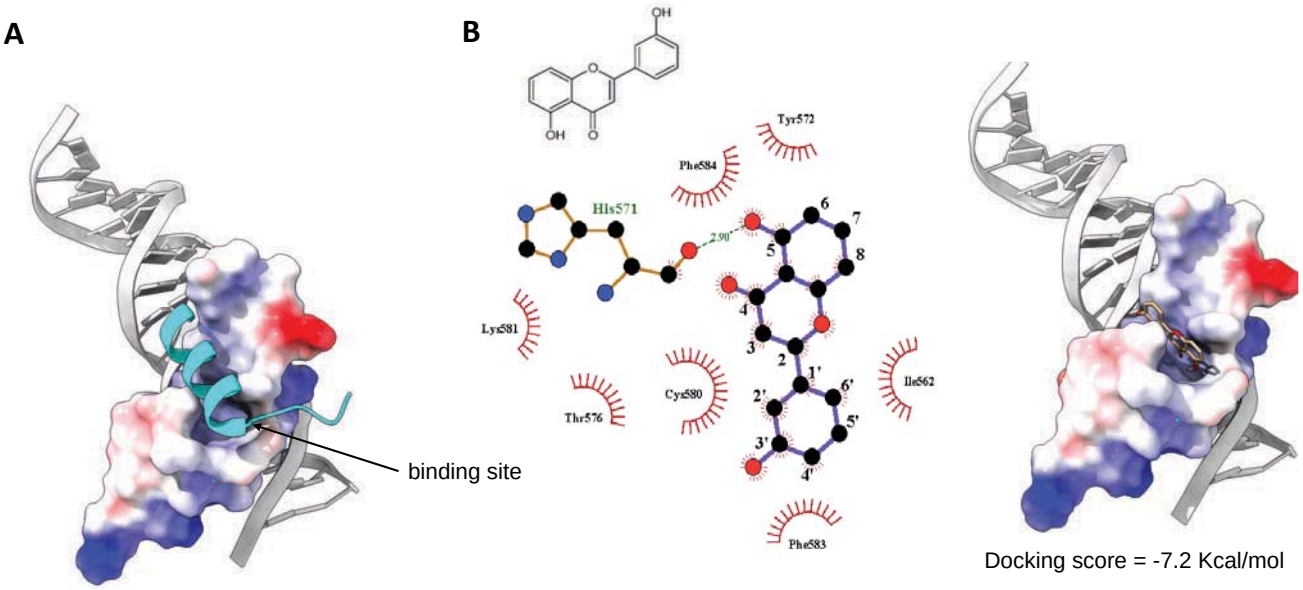

Figure 7

Downloaded from molpharm.aspetjournals.org at ASPET Journals on July 7, 2023